Arch. Metall. Mater. **64** (2019), 3, 1175-1182

DOI: 10.24425/amm.2019.129510

MISSAM IRANI*, MANSOO JOUN**#

PRACTICAL APPROACH TO DETERMINING DYNAMIC RECRYSTALLIZATION PARAMETERS USING FINITE ELEMENT OPTIMIZATION OF BACKWARD EXTRUSION PROCESS

In this study, we present a new method for obtaining the parameters of the Johnson-Mehl-Avrami-Kolmogorov equation for dynamic recrystallization grain size. The method consists of finite-element analysis and optimization techniques. An optimization tool iteratively minimizes the error between experimental values and corresponding finite-element solutions. Isothermal backward extrusion of the AA6060 aluminum alloy was used to acquire the main parameters of the equation for predicting DRX grain size. We compared grain sizes predicted using optimized and reference parameters with experimental values from the literature and found better agreement when the optimized parameters were applied.

Keywords: Dynamic recrystallization; Grain size; Optimization; Simulation

1. Introduction

The mechanical properties of polycrystalline metals are mainly controlled by the size and shape of the grains in microstructure. The ability to predict and control grain size and morphology during different metal forming processes thus allows the development of tailored material properties and optimized products [1]. Dynamic recrystallization (DRX) [2-4], meta-dynamic recrystallization [5-7], and static recrystallization [8,9] are the main mechanisms of grain evolution for hot metal forming processes. Among these, DRX is the dominant phenomenon for refining initially coarse grains [10]. Various types of empirical, semi-empirical, and mesoscopic models of grain evolution have been applied to predict DRX grain size [11-16]. Phenomenological modeling is an empirical approach that has been employed frequently [17-20]. In this approach, the results of observed phenomena are expressed as equations, regardless of the physical background. The coefficients of the equations in the model are typically obtained from experimental observation using regression techniques [18]. The kinetics of isothermal transformations have been described by the Johnson-Mehl-Avrami-Kolmogorov (JMAK) phenomenological model since the 40's and many researchers have given a fundamental contribution to extend the range of applicability of the model [21]. The grain sizes after DRX were also classically described using the Johnson-Mehl-Avrami-Kolmogorov (JMAK) model [22-24], which gives acceptable results compared with other models. Nevertheless, it is often applied to only narrow ranges of process variables, such as the strain rate and deformation temperature [25]. Thus, DRX parameters in the JMAK model are strongly dependent on the process variables; as such, it is essential to perform a large number of hot compression tests for a range of temperatures and strain rates to acquire these parameters [26-28].

In this study, we present a new approach, based on a combination of finite-element analysis (FEA) and optimization techniques, to identify DRX parameters in the JMAK equations using a practical metal forming process. We used isothermal backward extrusion of the AA6060 aluminum alloy to investigate the feasibility and reliability of the approach. To obtain the parameters of the grain size equation, we minimized the gap between the target and predicted values using the optimization processes. Experimental values of grain size from the literature were used as the target values.

2. Methodology

Figure 1 shows a conceptual flow chart of the methodology for identifying the DRX parameters, i.e., to calculate the optimized DRX parameters of the grain size equation. For this purpose, a metal forming product was quenched rapidly just after being formed to halt microstructural evolution, and the grain sizes on a plane section were then measured at specific sample points, which were shared with the control points for finite-element predictions and parameter optimization. The measured grain size at the i^{th} sample point, denoted as $D_{drx,tar(i)}$, respectively, were applied as the associated target values in the

* GYEONGSANG NATIONAL UNIVERSITY, GRADUATE SCHOOL OF MECHANICAL AND AEROSPACE ENGINEERING, JINJU-CITY, 664-953, REPUBLIC OF KOREA
** GYEONGSANG NATIONAL UNIVERSITY, RECAFT, SCHOOL OF MECHANICAL AND AEROSPACE ENGINEERING, JINJU-CITY, 664-953, REPUBLIC OF KOREA
# Corresponding author: msjoun@gnu.ac.kr

root mean square error formula [29] to define the following objective function:

$$\varphi = \sqrt{\frac{1}{n}\sum_{i=1}^{n}\left(D_{drx,tar(i)} - D_{drx,pre(i)}\right)^2} \quad (1)$$

where $D_{drx,pre(i)}$ is the finite element solutions of the grain size at the *ith* sample point, φ is the average of differences between the measured and predicted DRX grain size at the sample points. The objective function was optimized to minimize the differences between the predicted and associated measured values. Any empirical or theoretical models, including the JMAK model, can be used to predict the grain sizes. The experimental DRX grain size values [20] were considered to be the target grain sizes.

In the JMAK model [30], the the grain size after DRX, D_{drx}, was calculated as follows:

$$D_{drx} = b\, d_0^h \varepsilon^n \dot{\varepsilon}^m \exp\left(\frac{Q}{RT}\right) + c \quad (2)$$

where $\varepsilon, d_0, \dot{\varepsilon}, Q, R$ and T are effective strain, initial grain size, effective strain rate, activation energy of recrystallization, gas constant, and temperature, respectively. b, h, n, and m are the coefficients of the grain size equation. In this study, b, m, n, and Q are considered the design parameters. The optimization problems are thus defined by determining the design parameters that minimize the objective function φ, subject to inequality constraints, which are functions of the design variables and state variables including temperature.

The objective of the optimization process shown in Figure 1 is to find the DRX parameters, or design parameters, in an itera-

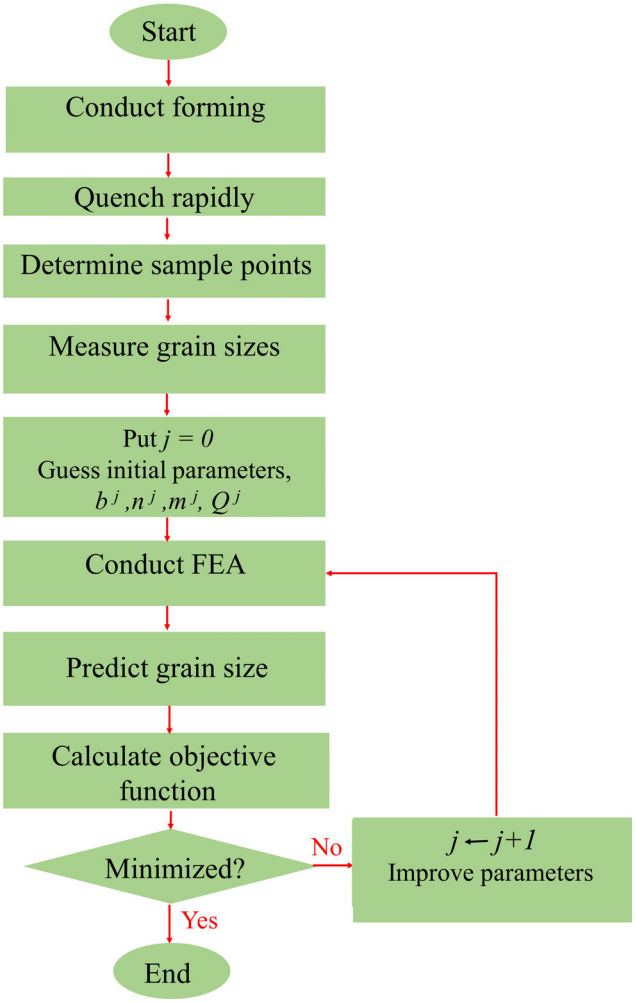

Fig. 1. Conceptual flow chart of the presented methodology

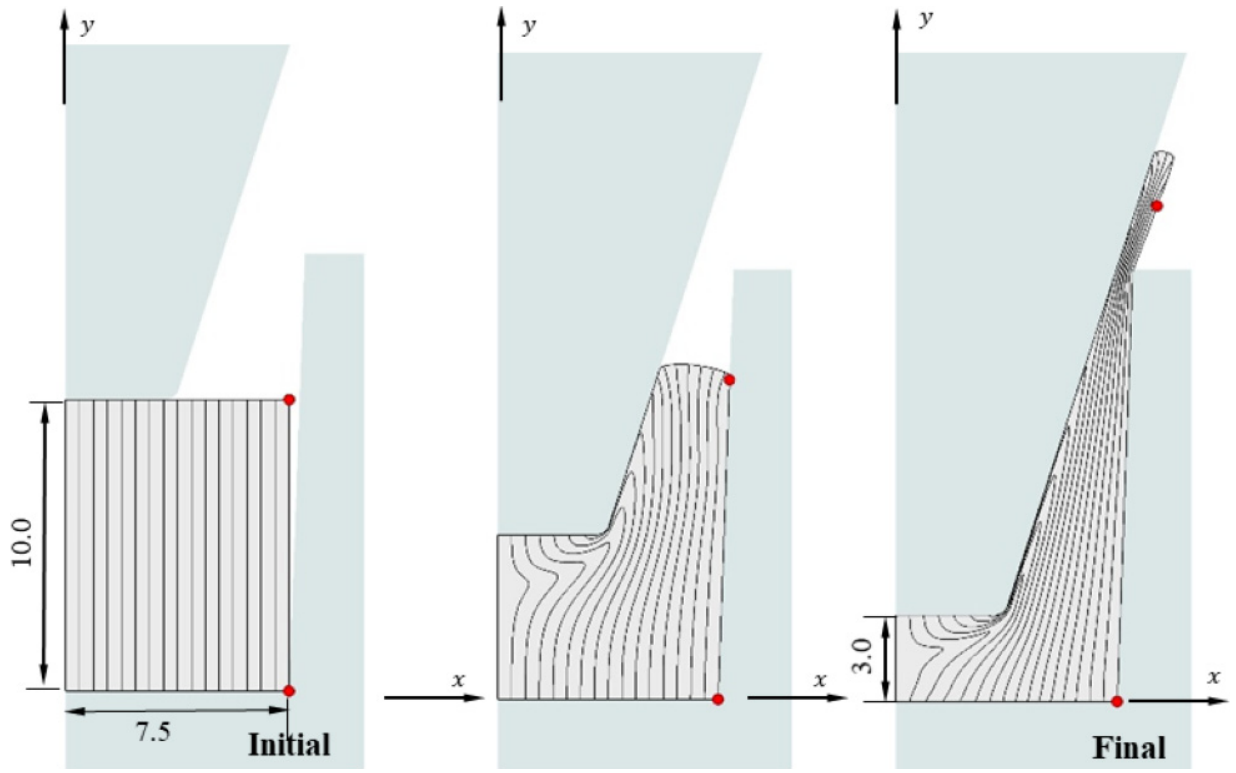

Fig. 2. Schematic diagram of the backward extrusion process (dimensions in mm)

tive way that predicts the grain sizes that are closest to the target values in terms of the objective function defined in Eq. (1). In the first step, an initial guess of the design parameters was made and the optimization procedure started from a FEA of the process with these initial values. The global response surface method (GRSM) [31] was used as the optimization technique. GRSM is a response surface-based approach that generates a few designs per iteration. Additional designs were generated globally to guarantee a good balance between local and global search capabilities. To provide a better fit of the model, the response surface was updated adaptively with the newly generated designs [32].

4. Application of the method

The validity of the method for obtaining the parameters of the grain size equation (Eq. 2) has been shown by the authors previously [33-36]. In the current study, the method is applied to acquire the parameters of the grain size equation practically. For this purpose, we examined isothermal backward extrusion of AA6060 aluminum alloy (chemical composition is given in Table 1) at 250, 450, and 550°C, and die velocities (v) of 0.1 and 5.0 mm/s as depicted in Figure 2.

TABLE 1

Chemical composition of the studied aluminum alloy

Si	Fe	Cu	Mn	Mg	Zn	Cr	Ti
0.43	0.21	0.02	0.03	0.48	0.02	0.0012	0.01

A finite-element simulation of the backward extrusion process was conducted using a commercial forging simulator AFDEX [37-40]. The elements size has a significant effect on optimization time. Thus, it is of great importance to determine the minimum number of element that not only ensures calculation accuracy but also saves optimization time [33]. The finite-element analysis with 2,000 quadrilateral elements was employed as shown in Figure 3. The temperature at the boundaries was constant to satisfy the isothermal condition. The flow stress of the alloy at hot working conditions is given to the simulation using the stress-strain curves at different temperature and strain rates [41]. A friction factor value (m = 0.22) was applied based on the ring test results [20].The grain sizes reported by Donati et al. [20] were used as the target values, $D_{drx,tar}$, in the objective function (Eq. 1). These grain sizes were measured at nine sample points on the cross-section of a workpiece at the final stroke of the process with two formation rates. Measured grain sizes are average values for a small area [42]; thus, we calculated the average of nodal values in a circle with a diameter of 900 μm to obtain the predicted grain size, $d_{\mathrm{DRX},pre}$, at each sample point (Fig. 3). The target values for different temperatures and die velocities are given in Table 2; these are the experimental values of the DRX grain size at the sample points [20].

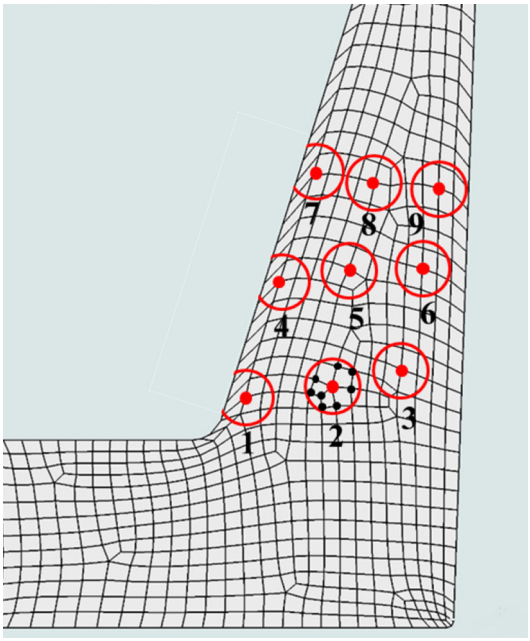

Fig. 3. Grain size sample points

To simplify the optimization problem, h and c were given values of 1 and 0, respectively. The optimization variables in Eq. (2) were b, m, n, and Q. The initial grain size, d_0, and the gas constant, R, were assigned values of 137 μm and 8.314472 J/kmol, respectively [30]. The constraints and the initial guesses for the optimization are listed in Table 3. The optimizations continued, until the iteration at which no additional decrease in the objective function was achieved (Fig. 4).

TABLE 2

Coordinates of the centers of circles at sample points and the corresponding target grain size

Sample point	x (mm)	y (mm)	Grain size (μm)					
			250°C, 0.1 mm/s	250°C, 5.0 mm/s	450°C, 0.1 mm/s	450°C, 5.0 mm/s	550°C, 0.1 mm/s	550°C, 5.0 mm/s
1	4.10	3.58	29	29	31	34	48	61
2	5.50	3.90	77	78	76	59	53	86
3	6.88	3.87	90	85	98	92	65	109
4	4.72	5.50	27	17	43	40	—	47
5	5.87	5.69	74	66	—	—	55	—
6	7.17	5.60	92	86	81	78	74	86
7	5.26	7.21	32	32	62	35	—	—
8	6.14	7.50	67	65	—	51	70	85
9	7.24	7.41	95	85	78	70	—	81

TABLE 3

Constraints and initial guesses of optimization variables at different temperatures

Temperature (°C)	Constraints	Initial guess
250	$1.0 \times 10^{15} < b < 1.0 \times 10^{17}$	$b^0 = 5.0 \times 10^{16}$
450	$1.0 \times 10^{10} < b < 1.0 \times 10^{12}$	$b^0 = 5.0 \times 10^{11}$
550	$1.0 \times 10^{8} < b < 1.0 \times 10^{10}$	$b^0 = 5.0 \times 10^{9}$
All temperatures	$-2.0 < m < 0.5$	$m^0 = -0.5$
	$-2.0 < n < 0.0$	$n^0 = -0.5$
	$150 < Q < 200$	$Q^0 = 175$ (kJ/mol)

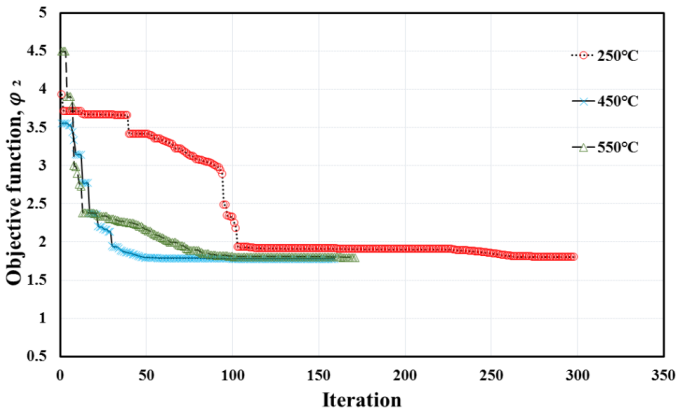

Fig. 4. Variation of the objective function with iterations at different temperatures

5. Results and discussion

The optimized DRX grain size parameters are compared with reference values [20,30] in Table 4. The parameter values were similar at 550°C. The obtained values for m at 250 and 450°C were also similar to the associated reference values, whereas the optimized and reference values of b and n differed. The values of Q obtained via optimization were in good agreement with the reference value of 161 kJ/mol.

Figures 5-7 illustrate the grain sizes predicted using reference and optimized DRX parameters at different die velocities and temperatures. The predicted grain size contours were similar at 550°C, due to comparable values of optimized and reference parameters (Table 4), whereas the greatest dissimilarities were observed at 250 °C for both forming rates. Figure 8 compares the measured grain sizes after DRX at 250°C with grain sizes predicted using both optimized and reference DRX parameters. The graphs show fewer differences at both formation rates. The results for 450°C are shown in Figure 9; predictions using the optimized parameters provided more accurate results, except at sample points 1 and 2, at a formation rate of 0.1 mm/s, and sample points 2 and 7 at a formation rate of 5.0 mm/s. The predicted and experimental grain sizes at 550°C are shown in Figure 10, which indicates similar predicted grain sizes using optimized and reference parameters; this result is consistent with the results represented in Figure 7.

To quantitatively investigate the accuracy of predicted grain size, we calculated the error between the experimental and predicted values for the i^{th} sample point as

$$Error(i) = \left| \frac{D_{drx,\exp(i)} - D_{drx,pre(i)}}{D_{drx,\exp(i)}} \right| \times 100 \qquad (3)$$

where $D_{drx,\exp}$ and $D_{drx,pre}$ are the experimental and predicted grain sizes, respectively.

TABLE 4

Optimized and reference parameters for DRX grain size at different temperatures

Grain size parameter	250°C		450°C		550°C	
	Optimized	Reference	Optimized	Reference	Optimized	Reference
b	1.84×10^{15}	1.93×10^{15}	9.70×10^{11}	1.34×10^{11}	9.92×10^{9}	8.26×10^{9}
n	–0.813	–0.364	–0.551	–0.722	–0.430	–0.420
m	–0.197	–0.213	–0.084	–0.084	0.047	0.046
Q (kJ/mol)	161.2	161	161.8	161	162	161

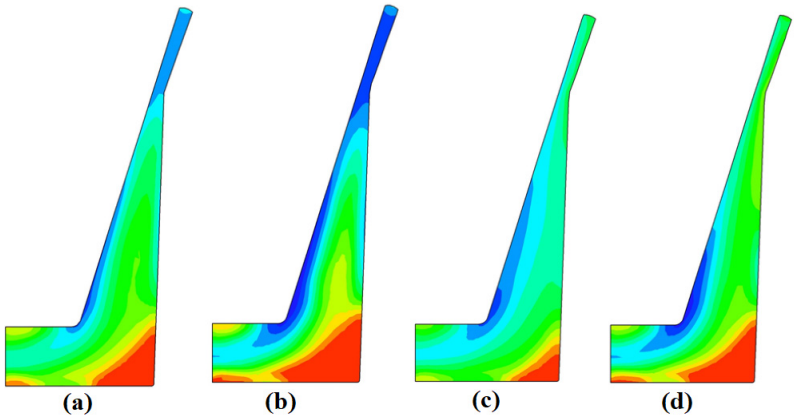

Fig. 5. Predicted DRX grain size (μm) at 250°C obtained using (a) reference parameters, $v = 0.1$ mm/s; (b) optimized parameters, $v = 0.1$ mm/s; (c) reference parameters, $v = 5.0$ mm/s; and (d) optimized parameters, $v = 5.0$ mm/s

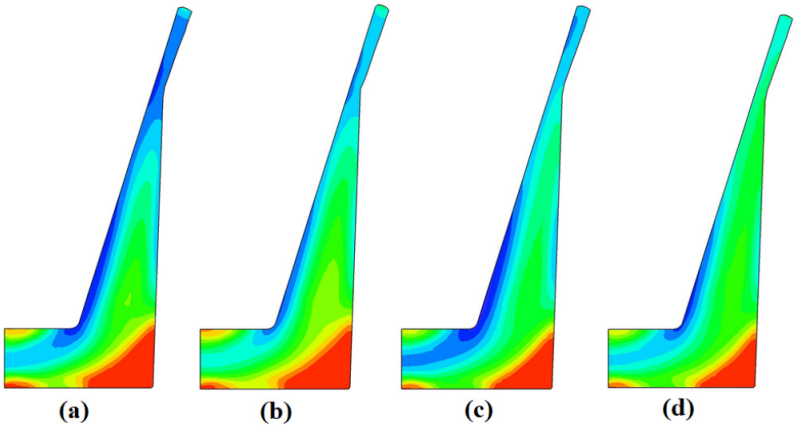

Fig. 6. Predicted DRX grain sizes (μm) at 450°C obtained using (a) reference parameters, v = 0.1 mm/s; (b) optimized parameters, v = 0.1 mm/s; (c) reference parameters, v = 5.0 mm/s; and (d) optimized parameters, v = 5.0 mm/s

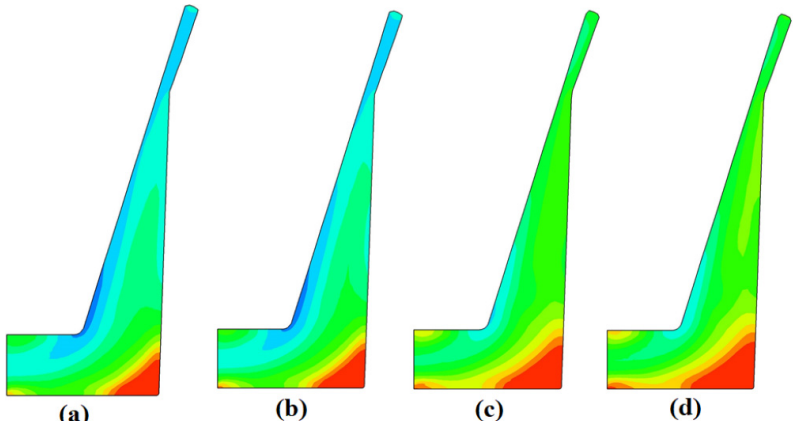

Fig. 7. Predicted DRX grain sizes (μm) at 550°C using (a) reference parameters, v = 0.1 mm/s; (b) optimized parameters, v = 0.1 mm/s; (c) reference parameters, v = 5.0 mm/s; and (d) optimized parameters, v = 5.0 mm/s

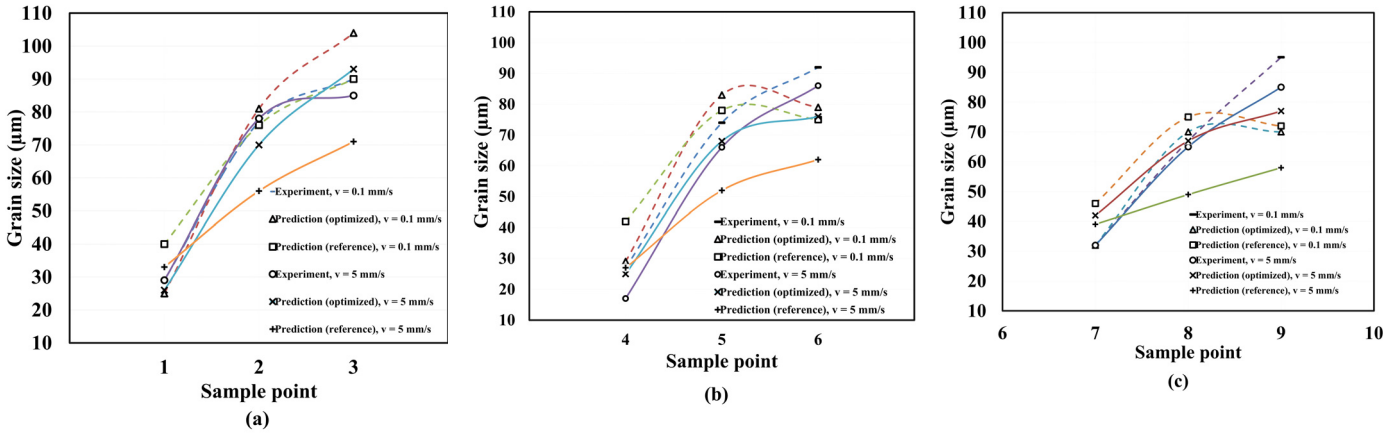

Fig. 8. Predicted and measured grain sizes at 250°C and sample points (a) 1 to 3 (b) 4 to 6 (c) 7 to 9

The variation in predicted grain size error at different temperatures is shown in Figs. 11-13. The maximum predicted grain size error obtained using the reference and optimized parameters were 58.8% and 47.1%, respectively. These large errors were found at lower temperature and in the upper section of the extruded cups, where tool misalignment can promote inhomogeneous deformation and non-symmetric wall thickness distribution in the workpiece [30].

The average error produced at different temperatures and formation rates is illustrated in Figure 14, showing that the optimized parameters provided a noticeable reduction in error compared with the reference parameters, especially at lower temperatures. However, the calculated average error of the optimized parameters was almost equal to that of the reference parameters at 550°C.

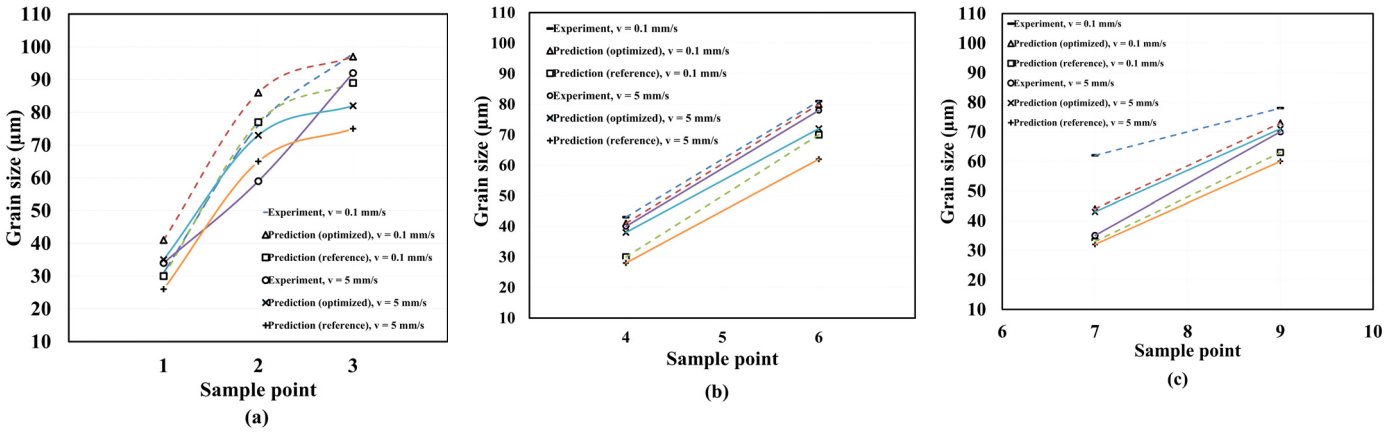

Fig. 9. Predicted and measured grain sizes at 450°C and sample points (a) 1 to 3 (b) 4 to 6 (c) 7 to 9

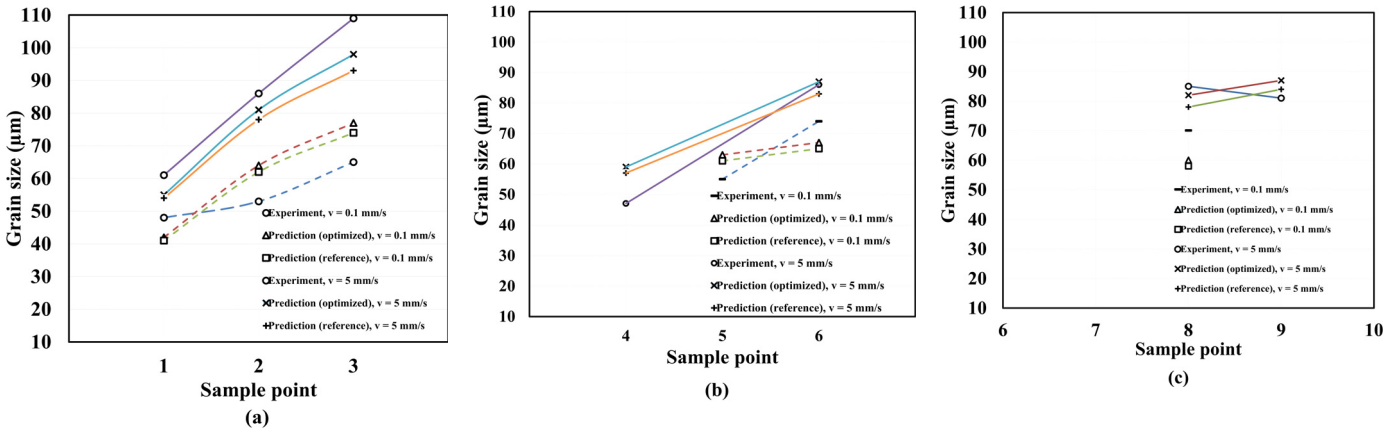

Fig. 10. Predicted and measured grain sizes at 550°C and sample points (a) 1 to 3 (b) 4 to 6 (c) 7 to 9

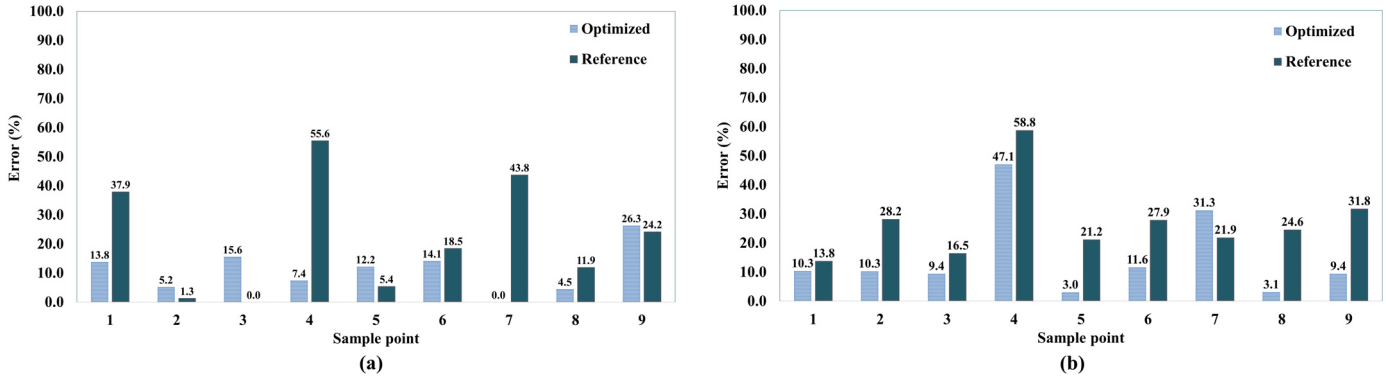

Fig. 11. Variation in predicted grain size error at 250°C at (a) v = 0.1 mm/s and (b) v = 5.0 mm/s

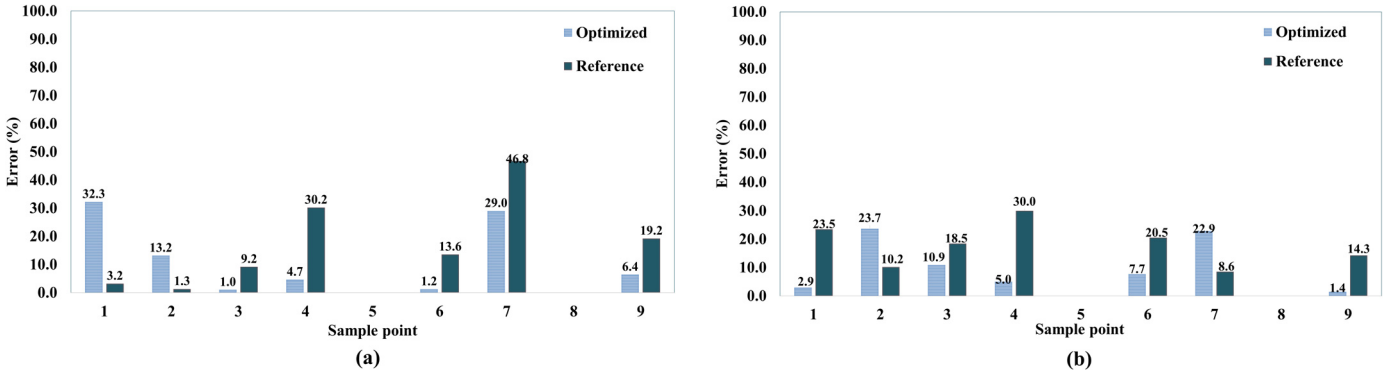

Fig. 12. Variation in predicted grain size error at 450°C at (a) v = 0.1 mm/s and (b) v = 5.0 mm/s

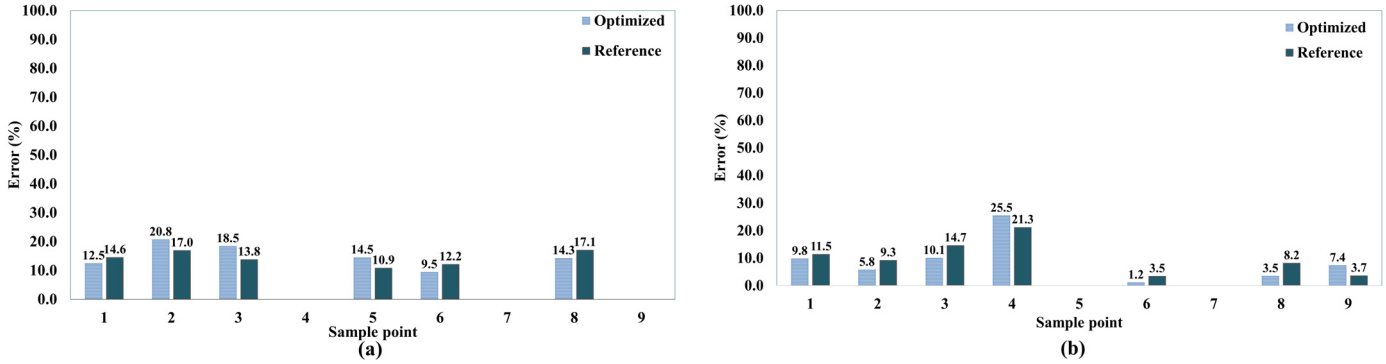

Fig. 13. Variation in predicted grain size error at 550°C at (a) v = 0.1 mm/s and (b) v = 5.0 mm/s

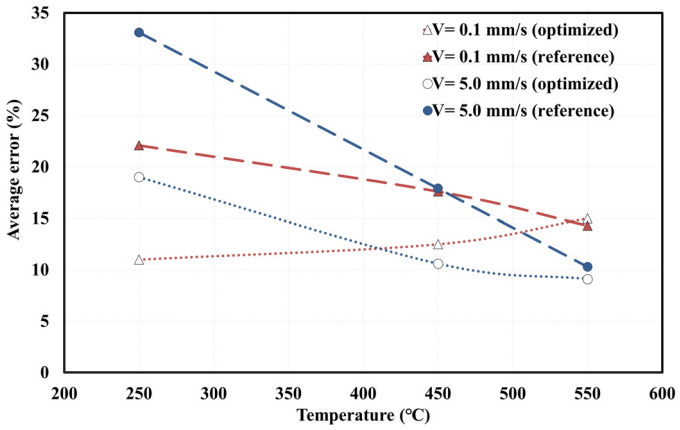

Fig. 14. Variation in average predicted grain size error at different deformation temperatures

6. Conclusion

In the present study, we described a practical method for determining DRX parameters using FEA optimization techniques. Optimized DRX parameters were acquired iteratively, minimizing the objective function of errors between target and predicted grain sizes at the sampled points. In this way, we obtained the main parameters in the JMAK equations for predicting the grain sizes. The method is economical because a large number of hot compression tests can be replaced by a simple and practical metal forming process such as extrusion, which was used in this study.

Comparing the predicted grain size using the reference and optimized parameters with the experimental grain size values indicated that the optimized parameters provided a significant reduction in error compared with that for the reference parameters, especially at lower temperatures.

Acknowledgement

This work is supported by the BK 21 plus, WC300 project for industry-university cooperative research of the Korean Small and Medium Business Administration.

REFERENCES

[1] H. Hallberg, Metals. **1**, 16-48 (2011).
[2] S. Naghdy, A. Akbarzadeh, Mater. Des. **53**, 910-914 (2014).
[3] H. Matsumoto, V. Velay, J. Alloys Compd. **708**, 404-413 (2017).
[4] H. Mirzadeh, M.H. Parsa, D. Ohadi, Mater. Sci. Eng. A. **569**, 54-60 (2013).
[5] Y.C. Lin, M.-S. Chen, Mater. Sci. Eng. A. **501**, 229-234 (2009).
[6] Y.C. Lin, L.-T. Li, Y.-C. Xia, Comput. Mater. Sci. **50**, 2038-2043 (2011).
[7] D.-G. He, Y.C. Lin, M.-S. Chen, L. Li, J. Alloys Compd. **690**, 971-978 (2017).
[8] M. Seyed Salehi, S. Serajzadeh, Comput. Mater. Sci. **53**, 145-152 (2012).
[9] Y.C. Lin, Y.-X. Liu, M.-S. Chen, M.-H. Huang, X. Ma, Z.-L. Long, Mater. Des. **99**, 145-152 (2016)
[10] F. Ren, F. Chen, J. Chen, Adv. Mater. Sci. Eng. **2014**, 1-16 (2014).
[11] Y.C. Lin, J. Zhang, J. Zhong, Comput. Mater. Sci. **43**, 752-758 (2008).
[12] A. Momeni, S.M. Abbasi, A. Shokuhfar, J. Iron Steel Res. Int. **14**, 66-70 (2007).
[13] R. Ebrahimi, S.H. Zahiri, A. Najafizadeh, J. Mater. Process. Technol. **171**, 301-305 (2006).
[14] Y.-C. Lin, M.-S. Chen, J. Zhang, Mater. Sci. Eng. A. **499**, 88-92 (2009).
[15] A. Cingara, H.J. McQueen, J. Mater. Process. Technol. **36**, 17-30 (1992).
[16] S.M. Abbasi, A. Shokuhfar, Mater. Lett. **61** (2007).
[17] F. Chen, Z. Cui, D. Sui, B. Fu, Mater. Sci. Eng. A. **540**, 46-54 (2012).
[18] F. Chen, Z. Cui, J. Chen, Manuf. Rev. **1**, 6 (2014).
[19] J. Liu, Z. Cui, L. Ruan, Mater. Sci. Eng. A. **529**, 300-310 (2011).
[20] L. Donati, J.S. Dzwonczyk, J. Zhou, L. Tomesani, Key Eng. Mater. **367**, 107-116 (2008).
[21] M. Fanfoni, M. Tomellini, Nuovo Cimento. **20**, 1171-1182 (1998).
[22] L. Fratini, G. Buffa, Int. J. Mach. Tools Manuf. **45**, 1188-1194 (2005).
[23] H.R.R. Ashtiani, P. Karami, Model. Numer. Simul. Mater. Sci. **05**, 1-14 (2015).
[24] L. Donati, A. Segatori, M. El Mehtedi, L. Tomesani, Int. J. Plast. **46**, 70-81 (2013).

[25] Y.-C. Lin, M.-S. Chen, J. Zhang, Mater. Sci. Eng. A. **499**, 88-92 (2009).
[26] Q. Zuo, F. Liu, L. Wang, C. Chen, Z. Zhang, Prog. Nat. Sci. Mater. Int. **25**, 66-77 (2015).
[27] H. Mirzadeh, M.H. Parsa, D. Ohadi, Mater. Sci. Eng. A. **569**, 54-60 (2013).
[28] J. Lin, J. Mater. Process. Technol. **143-144**, 281-285 (2003).
[29] J.-S. Chou, A.-D. Pham, Inf. Sci. **399**, 64-80 (2017).
[30] M. Schikorra, L. Donati, L. Tomesani, A.E. Tekkaya, J. Mater. Process. Technol. **201**, 156-162 (2008).
[31] J.P.C. Kleijnen, Simul. Model. Pract. Theory. **16**, 50-64 (2008).
[32] G. Gary Wang, Z. Dong, P. Aitchison, Eng. Optimiz. **33** (6), 707-733 (2007)
[33] M. Irani, M. Joun, Comput. Mater. Sci. **142**, 178-184 (2018).
[34] M. Irani, M. Joun, Practical Approach to Determining Material Parameters in Microstructure Evolution, in: The Korean Society for the Technology of Plasticity, 122-123 (2017).
[35] M. Irani, M. Joun, Obtaining parameters of dynamic recrystallization kinetics using FEM and optimization technique, in: The Korean Society for the Technology of Plasticity, 91-92 (2017).
[36] M. Irani, SG. Lim, M. Joun, Acquisition of Coefficients of JMAK Model for Microstructural Evolution using a Hot Forging Process of Outer Race, in: The Korean Society for the Technology of Plasticity, 140-141 (2018).
[37] J.G. Eom, Y.H. Son, S.W. Jeong, S.T. Ahn, S.M. Jang, D.J. Yoon, M.S. Joun, Mater. Des. **54**, 1010-1018 (2014).
[38] M. Joun, J.G. Eom, M.C. Lee, Mech. Mater. **40**, 586-593 (2008).
[39] M.C. Lee, S.H. Chung, S.M. Jang, M.S. Joun, Finite Elem. Anal. Des. **45**, 745-754 (2009).
[40] M.S. Joun, H.G. Moon, I.S. Choi, M.C. Lee, B.Y. Jun, Tribol. Int. **42**, 311-319 (2009).
[41] Y Prasad, KP Rao, S Sasidhar, hot working guide a compendium of processing maps, ASM international, 2015.
[42] C. Bandini, B. Reggiani, L. Donati, L. Tomesani, in: MADISON, Chicago IL, USA, 789-800 (2016).